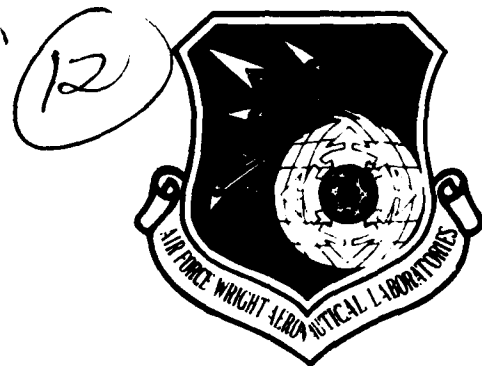




# AD A119829

AFWAL-TR-82-2042  
Volume II



MATERIAL CHARACTERIZATION, PART B MECHANICAL PROPERTIES  
OF TWO METAL MATRIX COMPOSITE MATERIALS

S. A. Emery

University of Dayton Research Institute  
Dayton, Ohio 45469

May 1982

Interim Report for Period 1 October 1977 - 30 June 1980

Approved for public release; distribution unlimited.

AERO PROPULSION LABORATORY  
AIR FORCE WRIGHT AERONAUTICAL LABORATORIES  
AIR FORCE SYSTEMS COMMAND  
WRIGHT-PATTERSON AIR FORCE BASE, OHIO 45433

DTIC FILE COPY

DTIC  
ELEC  
S OCT 4 1982  
A

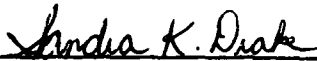
82 10 04 158

NOTICE

When Government drawings, specifications, or other data are used for any purpose other than in connection with a definitely related Government procurement operation, the United States Government thereby incurs no responsibility nor any obligation whatsoever; and the fact that the government may have formulated, furnished, or in any way supplied the said drawings, specifications, or other data, is not to be regarded by implication or otherwise as in any manner licensing the holder or any other person or corporation, or conveying any rights or permission to manufacture, use, or sell any patented invention that may in any way be related thereto.

This report has been reviewed by the Office of Public Affairs (ASD/PA) and is releasable to the National Technical Information Service (NTIS). At NTIS, it will be available to the general public, including foreign nations.

This technical report has been reviewed and is approved for publication.

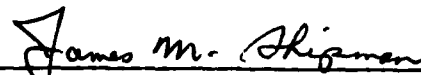


SANDRA K. DRAKE  
Project Engineer



ISAK J. GERSHON  
Technical Area Manager,  
Propulsion Mechanical Design

FOR THE COMMANDER



J. SHIPMAN, MAJ, USAF  
Deputy Director, Turbine Engine Division

"If your address has changed, if you wish to be removed from our mailing list, or if the addressee is no longer employed by your organization, please notify AFNAL/POTA, WPAFB OH 45433 to help us maintain a current mailing list."

Copies of this report should not be returned unless return is required by security considerations, contractual obligations, or notice on a specific document.

UNCLASSIFIED

SECURITY CLASSIFICATION OF THIS PAGE (When Data Entered)

REPORT DOCUMENTATION PAGE		READ INSTRUCTIONS BEFORE COMPLETING FORM
1. REPORT NUMBER AFWAL-TR-82-2042 Vol. II	2. GOVT ACCESSION NO. AD-A119829	3. RECIPIENT'S CATALOG NUMBER
4. TITLE (and Subtitle) MATERIAL CHARACTERIZATION, PART B MECHANICAL PROPERTIES OF TWO METAL MATRIX COMPOSITE MATERIALS	5. TYPE OF REPORT & PERIOD COVERED Technical Report Oct. 1977 - June 1980	
	6. PERFORMING ORG. REPORT NUMBER UDR-TR-80-37	
7. AUTHOR(s) S. A. Emery	8. CONTRACT OR GRANT NUMBER(s) 200-4BA-14K-47844 (GE) F33615-77-C-5221	
9. PERFORMING ORGANIZATION NAME AND ADDRESS University of Dayton Research Institute 300 College Park Ave. Dayton, Ohio 45469	10. PROGRAM ELEMENT, PROJECT, TASK AREA & WORK UNIT NUMBERS 62203F, 3066, 12, 33	
11. CONTROLLING OFFICE NAME AND ADDRESS General Electric Company Evendale Plant - Aircraft Engine Group Evendale, Ohio 45215	12. REPORT DATE May, 1982	
	13. NUMBER OF PAGES 40	
14. MONITORING AGENCY NAME & ADDRESS (if different from Controlling Office) Aero-Propulsion Laboratory Wright-Patterson Air Force Base Ohio 45433	15. SECURITY CLASS. (of this report) Unclassified	
	15a. DECLASSIFICATION/DOWNGRADING SCHEDULE	
16. DISTRIBUTION STATEMENT (of this Report)  Approved for public release; distribution unlimited.		
17. DISTRIBUTION STATEMENT (of the abstract entered in Block 20, if different from Report)		
18. SUPPLEMENTARY NOTES		
19. KEY WORDS (Continue on reverse side if necessary and identify by block number)  Stainless steel wire mesh, boron aluminum, foreign object damage, mechanical properties, unidirectional tests		
20. ABSTRACT (Continue on reverse side if necessary and identify by block number)  This report describes mechanical property data collected in support of a fan blade analysis model. The development of the blade model is part of a foreign object damage (FOD) study of jet engine fan blades. Use of the properties in the model allows one to evaluate potential fan blade materials. Part A of this report contains a discussion of the mechanical property tests conducted on two metallic materials: 410 stainless steel and		

DD FORM 1473  
1 JAN 73

UNCLASSIFIED  
SECURITY CLASSIFICATION OF THIS PAGE (When Data Entered)

UNCLASSIFIED

SECURITY CLASSIFICATION OF THIS PAGE(When Data Entered)

20.

8Al-1Mo-1V titanium. These two materials were selected because of their use in the J-79 blade and the F-101 blade, respectively. Part B of the report contains a discussion of mechanical property tests conducted on the two composite components of a hybrid composite blade: boron/2024 aluminum and stainless steel wire mesh/2024 Aluminum. These two composites are used in the hybrid composite APSI blade.

Quasi-static tensile tests and torsional tests were conducted on unidirectional specimens for the two composites indicated above. The mechanical properties calculated include the Young's moduli in the three principle directions, Poisson's ratio (when obtainable), the shear moduli, and ultimate strength and strain (both when obtainable).

A

UNCLASSIFIED

SECURITY CLASSIFICATION OF THIS PAGE(When Data Entered)

FOREWORD

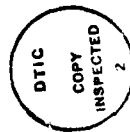
This report describes a contractual work effort conducted for the General Electric Company, Aircraft Engine Group under Purchase Order No. 200-4BA-14K-47844 which is a subcontract of F33615-77-C-5221.

This report covers work conducted during the period of October 1977 to June 1980 and is part of Task IV-A.

The GE Program Manager was Mr. Joe McKenzie and the Principal Investigator was Mr. Al Storace. The work reported herein was performed under the direction of Susan A. Emezy, Experimental and Applied Mechanics Division, University of Dayton Research Institute.

Technical support was provided by Mr. E. C. Klein. Program management for the University was provided by Mr. Robert Bertke.

This report covers work conducted for project 3066, task 12, entitled Foreign Object Impact Design Criteria. The contract was sponsored by the Aero Propulsion Laboratory, Air Force Systems Command, Wright-Patterson AFB, Ohio 45433 under the direction of Sandra K. Drake (AFWAL/POTA), Project Engineer.



DTIC	
ATIS GRAS1	<input checked="" type="checkbox"/>
DTIC PIP	<input type="checkbox"/>
Unannounced	<input type="checkbox"/>
Justification	
Distribution	
Availability Codes	
Dist	Special
A	

## TABLE OF CONTENTS

<u>SECTION</u>		<u>PAGE</u>
I	INTRODUCTION	1
II	DEFINITION OF THE TEST MATRIX	3
	2.1 LINEAR LAMINATE THEORY	3
	2.2 RATE OF TESTING	7
	2.3 SPECIMEN CONFIGURATION AND INSTRUMENTATION	9
	2.3.1 Modified IITRI Specimen	9
	2.3.2 Modified 10° Off-Axis Specimen	10
	2.3.3 Through-the-Thickness Specimen	15
	2.3.4 Torsion Rod Specimen	15
	2.3.5 <u>±</u> 45° Specimen	20
III	TEST FIXTURES AND EXPERIMENTAL PROCEDURES	22
	3.1 TEST FIXTURE AND PROCEDURES FOR 0° B/A1, 90° B/A1, 0-90° SSWM, 10° OFF-AXIS B/A1, and <u>±</u> 45° SPECIMENS	22
	3.2 TEST FIXTURE AND PROCEDURES FOR THE THROUGH-THE-THICKNESS SPECIMEN	25
	3.3 TEST FIXTURE AND PROCEDURES FOR THE SSWM AND B/A1 TORSION ROD SPECIMENS	25
IV	DATA REDUCTION	28
	4.1 MODIFIED IITRI SPECIMEN (0° B/A1, 90° B/A1, and 0-90° SSWM)	28
	4.2 <u>±</u> 45° SSWM SPECIMEN	29
	4.3 THROUGH-THE-THICKNESS SPECIMEN	30
	4.4 10° OFF-AXIS SPECIMEN	30
	4.5 TORSION ROD SPECIMEN	32
V	RESULTS AND CONCLUSIONS	33
VI	REFERENCES	40

LIST OF ILLUSTRATIONS

<u>FIGURE</u>		<u>PAGE</u>
1	Principal and Shear Directions Relative to Boron/2024 Aluminum Unidirectional Specimens.	5
2	Principal and Shear Directions Relative to Stainless Steel Wire Mesh Unidirectional Specimens.	6
3	Specimen Configuration for 0° Boron/2024 Aluminum.	11
4	Specimen Configuration for 90° Boron/2024 Aluminum.	12
5	Specimen Configuration for 0/90° Stainless Steel Wire Mesh/2024 Aluminum.	13
6	Specimen Configuration for 10° Off-Axis Boron/2024 Aluminum.	16
7	Specimen Configuration for Through-The-Thickness Stainless Steel Wire Mesh/2024 Aluminum.	17
8	Specimen Configuration for Rod Torsion Stainless Steel Wire Mesh/2024 Aluminum.	18
9	Specimen Configuration for Rod Torsion Boron/2024 Aluminum.	19
10	Specimen Configuration for + 45° Stainless Steel Wire Mesh/2024 Aluminum.	21
11	Test Fixture Used to Test All Flat Specimens with Specimen Installed.	23
12	Entire Test System Used to Conduct All Tests for This Report Except the Rod Torsion Tests.	24
13	Test Fixture for Through-The-Thickness Specimen with Specimen Installed.	26
14	Test Fixture for Rod Torsion Tests Shown with Specimen Installed.	27

LIST OF TABLES

<u>TABLE</u>		<u>PAGE</u>
1	COMPOSITE MATERIAL TEST MATRIX	3
2	AVERAGED ELASTIC MECHANICAL PROPERTIES FOR B/2024 Al and SSWM.	33
3	RESULTS FROM 0° B/Al MODIFIED IITRI SPECIMEN	34
4	RESULTS FROM 90° B/Al MODIFIED IITRI SPECIMEN	34
5	RESULTS FROM 0/90° SSWM MODIFIED IITRI SPECIMEN	35
6	RESULTS FROM THE THROUGH-THE-THICKNESS SPECIMEN	35
7	RAW AND REDUCED DATA FROM $\pm$ 45° SSWM SPECIMEN	36
8	RECORDED AND REDUCED DATA FROM 10° OFF-AXIS B/Al SPECIMENS	37
9	RECORDED DATA AND CALCULATED RESULTS FROM TORSION ROD SPECIMEN	38

SECTION I  
INTRODUCTION

Foreign objects (ice balls, ice spears, and small birds) cause considerable damage when they impact jet engine fan blades at particular angles and velocities. Rapidly rising material and production costs make repairs quite expensive. Such costs also make experimentation with new blade designs and materials excessively expensive. This necessitates the developments of design techniques (for designing foreign object damage [FOD] resistant fan blades) that require minimal testing of actual parts prior to determining the optimum combination of blade shape and material properties. An FOD contractual effort aimed at providing the described design capability has concentrated on two items: (1) producing a fan blade analytical model and (2) understanding FOD failure mechanisms. The availability of these techniques will greatly enhance the possibility of using composite materials in jet engines (which is desirable because of their high strength to density ratio).

The fan blade analysis model requires as an input the mechanical properties of the material used in the modeled blade. In the present FOD research program three existing blades were studied: the J-79 blade, the F-101 blade and the APSI blade. As part of the research, the mechanical properties were obtained for the materials involved: 410 stainless steel (used in the J-79 blade), 8Al-1Mo-1V titanium (used in the F-101 blade), and boron/2024 aluminum and stainless steel wire mesh (both used in the APSI blade). The tests on the two metallic materials were conducted at several strain ratios are discussed in the report entitled "Material Characterization: Part A". The present report, "Material Characterization: Part B", contains a discussion of the mechanical property tests of the two metal matrix composite materials.

Although the hybrid composite APSI blade has a complex ply construction, the mechanical properties presented in this report were obtained using simplified specimens made with the most basic fiber configuration for each material. The unidirectional boron aluminum specimens supplied these elastic parameters:  $E_1$ ,  $E_2 (=E_3)$ ,  $\nu_{12}$ ,  $G_{12} (=G_{31})$ , and  $G_{23}$ . The 0 and 90° "unidirectional" stainless steel wire mesh (SSWM) specimens gave values for  $E_1 (=E_2)$ ,  $E_3$ ,  $\nu_{12}$ ,  $G_{12}$ , and  $G_{23} (=G_{31})$ . Laminate theory can be used to calculate the bulk properties of the blade which has the following ply layup: SSWM/0° B-Al/22° B-Al/0° B-Al/-22° B-Al/SSWM/Al/SSWM/-22° B-Al/0° B-Al/22° B-Al/0° B-Al/SSWM. The matrix material in both composite subsystems was 2024 aluminum. The bulk properties were not calculated for this report. The tests were conducted at one strain rate, 0.001 strain/second, because based on research conducted by Krinke, Barber, and Nicholas<sup>(1)</sup> the assumption was made that these composite materials would not be strain rate dependent. The materials tested had approximately a 40 percent fiber volume content.

SECTION II  
DEFINITION OF THE TEST MATRIX

This section contains a discussion of several criteria used to establish the test matrix for the composite material tests. The matrix appears in Table 1. Items considered include the availability of laminate theory, a previous study of the strain rate dependence of boron/6061 aluminum, and the selection of technically acceptable test specimen configurations and instrumentation.

TABLE 1. COMPOSITE MATERIAL TEST MATRIX

Material	Specimen Configuration	Fiber Orientation to Load Axis	Parameter Obtained
Boron/ 2024 Aluminum	IITRI	0°	$E_1, \nu_{12}$
	"	90°	$E_2 (=E_3)$
	10° off-axis	10°	$G_{12} (=G_{31})$
	Torsion	90°	$G_{23}$
Stainless Steel Wire Mesh/2024 Aluminum	IITRI	0/90°	$E_1 (=E_2), \nu_{12}$
	+45°	+45°	$G_{12}$
	Through-the-thickness	90°	$E_3$
	Torsion	90°	$G_{23} (=G_{31})$

2.1 LINEAR LAMINATE THEORY

Linear laminate theory utilizes the properties obtained from unidirectional composite specimens to predict section properties of more complex fiber lay-ups. The hybrid composite APSI blade readily lends itself to the use of laminate theory for two reasons. First, the blade consists of two metal matrix composites: stainless steel wire mesh-2024 aluminum (SSWM) and boron-2024 aluminum (B/Al). The complex ply sequence follows for half of the blade thickness (where SSWM was the outer most

ply): SSWM/0° B-Al/22° B-Al/0°B-Al/-22°B-Al/SSWM/Al. The remaining half of the blade is a mirror image of this sequence. Second, as can be seen from the preceding sequence, the lay-up of the B/Al was not simple either.

Both the SSWM and the B/Al are anisotropic materials which implies that the mechanical properties each must be independently obtained in relation to all three principle directions. Figures 1 and 2 show schematics of the fiber and ply orientation with respect to the material principle axes of the B/Al and the SSWM, respectively. Three normal and three shear directions are indicated. The two paragraphs that follow discuss the fact that both composite materials exhibit some symmetry. This eliminates the need to test individually for all the following elastic parameters:  $E_1$ ,  $E_2$ ,  $E_3$ ,  $G_{12}$ ,  $G_{23}$ , and  $G_{31}$ .

The diagrams in Figure 1 represent the boron aluminum. A load applied in the one direction yields mechanical properties that are primarily influenced by the boron fibers. Properties obtained by applying a load in either the two or three direction would be characteristic of the matrix material, 2024 aluminum. In other words,  $E_2 = E_3$  for this material. Similarly,  $G_{12}$  and  $G_{31}$  are assumed to be equal because the properties of the fibers in the test specimens predominate over those of the matrix. In the B/Al,  $G_{23}$  is primarily representative of the matrix material.

The diagrams in Figure 2 represent the stainless steel wire mesh. For this material the characteristics of the stainless steel fibers predominate for loads applied in the one and two directions. Assuming that the warp and fill direction fibers have the same configuration then  $E_1 = E_2$  for this material. The matrix material, 2024 aluminum, has prime influence on  $E_3$ . The assumption that  $G_{23} = G_{31}$  for this material comes from the symmetry provided by fibers in both the 0° and 90° directions.  $G_{12}$  must be calculated from a separate test.

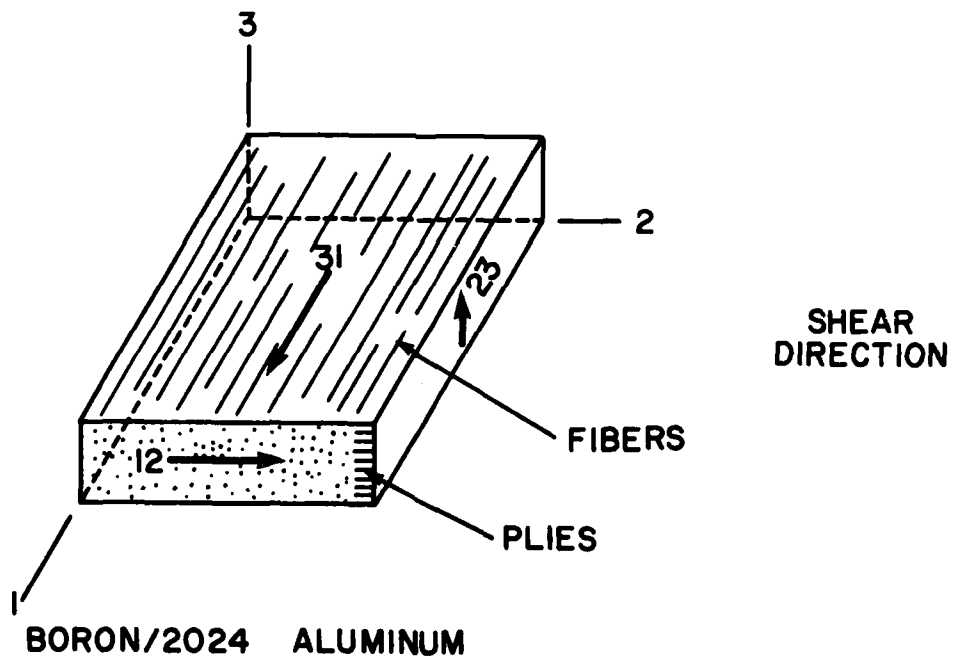
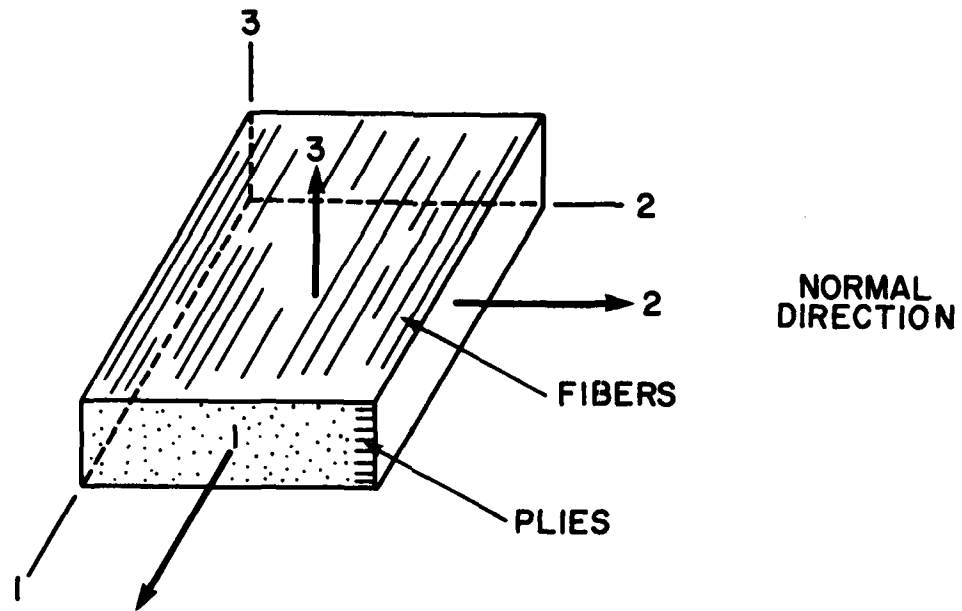
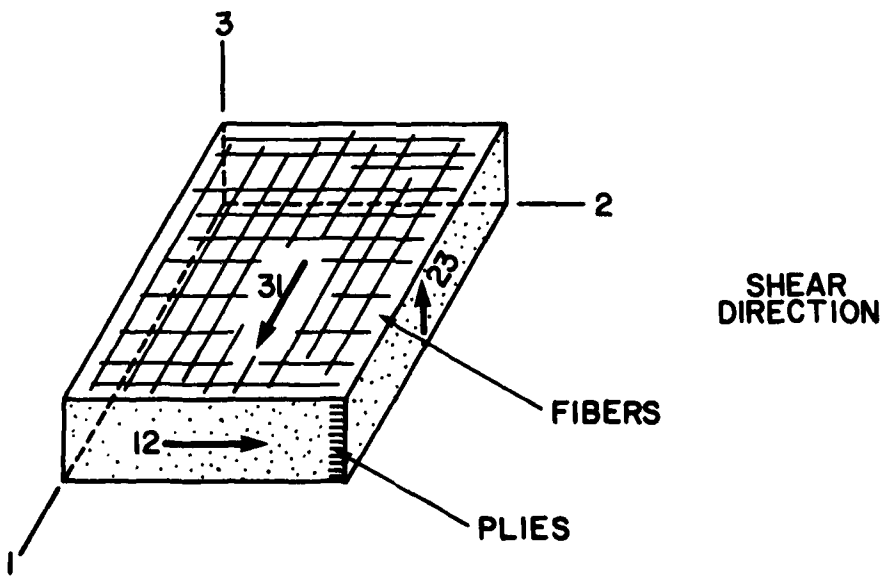
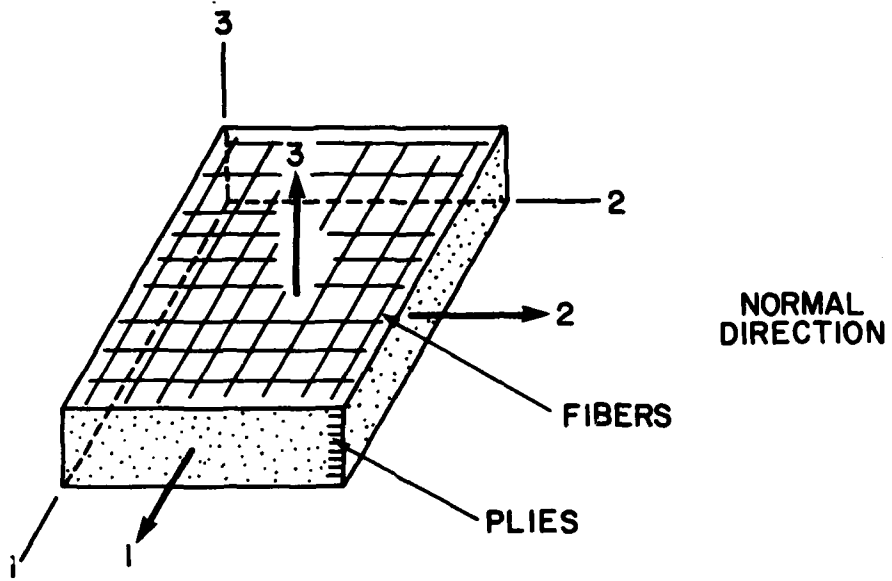


Figure 1. Principal and Shear Directions Relative to Boron/2024 Aluminum Unidirectional Specimens.



**STAINLESS STEEL WIRE MESH**

Figure 2. Principal and Shear Directions Relative to Stainless Steel Wire Mesh Unidirectional Specimens.

In summary, the partial symmetry in each of the materials reduced the types of specimens required to obtain the desired mechanical properties of these materials. The parameters  $E_1$ ,  $E_2$ ,  $\nu_{12}$ ,  $G_{12}$ , and  $G_{23}$  needed to be independently obtained for the boron aluminum while  $E_1$ ,  $E_3$ ,  $\nu_{12}$ ,  $G_{12}$ , and  $G_{23}$  had to be acquired for the stainless steel wire mesh.

## 2.2 RATE OF TESTING

The influence of strain rate on the mechanical properties of fan blade materials is an important consideration in FOD studies because of the range of strain rates produced in the blade by a variety of impact loads and velocities. The metallic material characterization tests, discussed in Part A of this report, were conducted at several testing rates. Most of their mechanical properties depended to some extent on the testing rate. However, the composite material characterization tests described in this volume (Part B) of the report were to be conducted at one testing rate. The following paragraphs describe the reasons for that decision.

The fabrication costs of metal matrix composite specimens prohibit unnecessary extensive testing of the subject materials. An inspection of various studies<sup>(1,2,3,4)</sup> revealed that the mechanical properties of these material systems (boron, several B/Al composites, and several aluminum alloys) were not strain rate dependent at ambient temperatures (72° to 75°F) over several decades of strain rate. The first three investigations describe conventional tension and/or compression tests conducted on unidirectional boron composites<sup>(1,2)</sup> or on aluminum alloys<sup>(3)</sup>. The tests encompassed six decades of strain rate ( $10^{-3}$  to  $10^2$  strain/sec) and all indicated little or no strain rate dependence of the materials involved. The fourth study (by Krinke, Barber and Nicholas), described below because the three point bend tests used are not conventional mechanical property tests, also indicated no significant strain rate dependence over six decades of strain

rate. Based on the cited works (concerning boron and aluminum) and discussions with the sponsor of the current effort (in which the sponsor indicated that they did not expect the SSWM to be strain rate dependent) the University decided to conduct the composite material characterization tests at the strain rate of 1 strain/sec. While running the tests it was decided that a strain rate of 0.001 strain/sec was more desirable.

The purpose of the Krinke work was to evaluate the Charpy impact test as a method for screening composite materials for impact resistance. Three point bend tests conducted on three materials (boron/6061 aluminum, boron/1100 aluminum, and graphite/epoxy) provided load-deflection curves and energy absorption data. The data, obtained at three displacement rates (0.002 in/sec, 1 in/sec and 100 in/sec), was compared to stresses and deflections predicted by strength of materials formulas and by more sophisticated theory of elasticity solutions. For additional information from the study, the ultimate bending strength and the energy absorption were both plotted versus strain rate. Since only one test was conducted per material per specimen depth per testing rate, the data showed considerable scatter. A plot of the averaged ultimate bending strength (from tests on specimens of different thicknesses) versus strain rate for the three materials showed a general trend of a slight increase in bending strength for an increase in strain rate. The rate of increase was about 1 percent per decade of strain rate for the boron/6061-aluminum and 2 percent per decade of strain rate for the boron/1100-aluminum. The conclusion reached in the present study about the Krinke work was that the rate of increase of the ultimate bending strength with strain rate was insignificant for the boron/aluminum materials over the tested range of six decades of strain rate.

As indicated above, the University planned to execute the test matrix shown in Table 1 at the displacement rate of 1 in/sec. This displacement rate corresponds to strain rates between 0.33 and 2 strain/sec for the various specimen configurations,

depending on the specimen gage length. A few tests on boron aluminum were conducted at this rate. However, mechanical properties significantly lower than expected were calculated from the results. Consequently, several tests were conducted at a displacement rate of 0.001 in/sec to enable close observation of the specimen during the test. Comparable values were obtained for both rates so the remainder of the tests were conducted at the slower rates for two reasons. First, each specimen could be closely observed during the entire test. Secondly, the data could be recorded directly on the X-Y recorders, thus producing smoother curves (than can be obtained from data recorded digitally and played back) for data analysis purposes.

### 2.3 SPECIMEN CONFIGURATION AND INSTRUMENTATION

The following paragraphs describe and justify the specimen configurations selected to obtain the parameters specified in Table 1. The included specimen illustrations have the nominal dimensions indicated. The transducers used to measure the strains (various high resistance foil strain gages) on each specimen type are mentioned. The analysis of the data is briefly described in Section IV.

#### 2.3.1 Modified IITRI Specimen

A modified IITRI (Illinois Institute of Technology Research Institute) specimen was used for three test types: the 0° B/Al, the 90° B/Al, and the 0/90° SSWM. The Structural Design Guide for Advanced Composite Applications recommends the IITRI configuration for obtaining unidirectional mechanical properties of composite materials. The fibers in the IITRI specimens are parallel and/or perpendicular to the applied load. The Guide indicated that the specimen is particularly useful for testing organic matrix composites. Consequently, the University assumed that the configuration was also acceptable for testing metal matrix composites. For the current program the following two modifications were made (and justified by the fact that the matrix material was metallic rather than

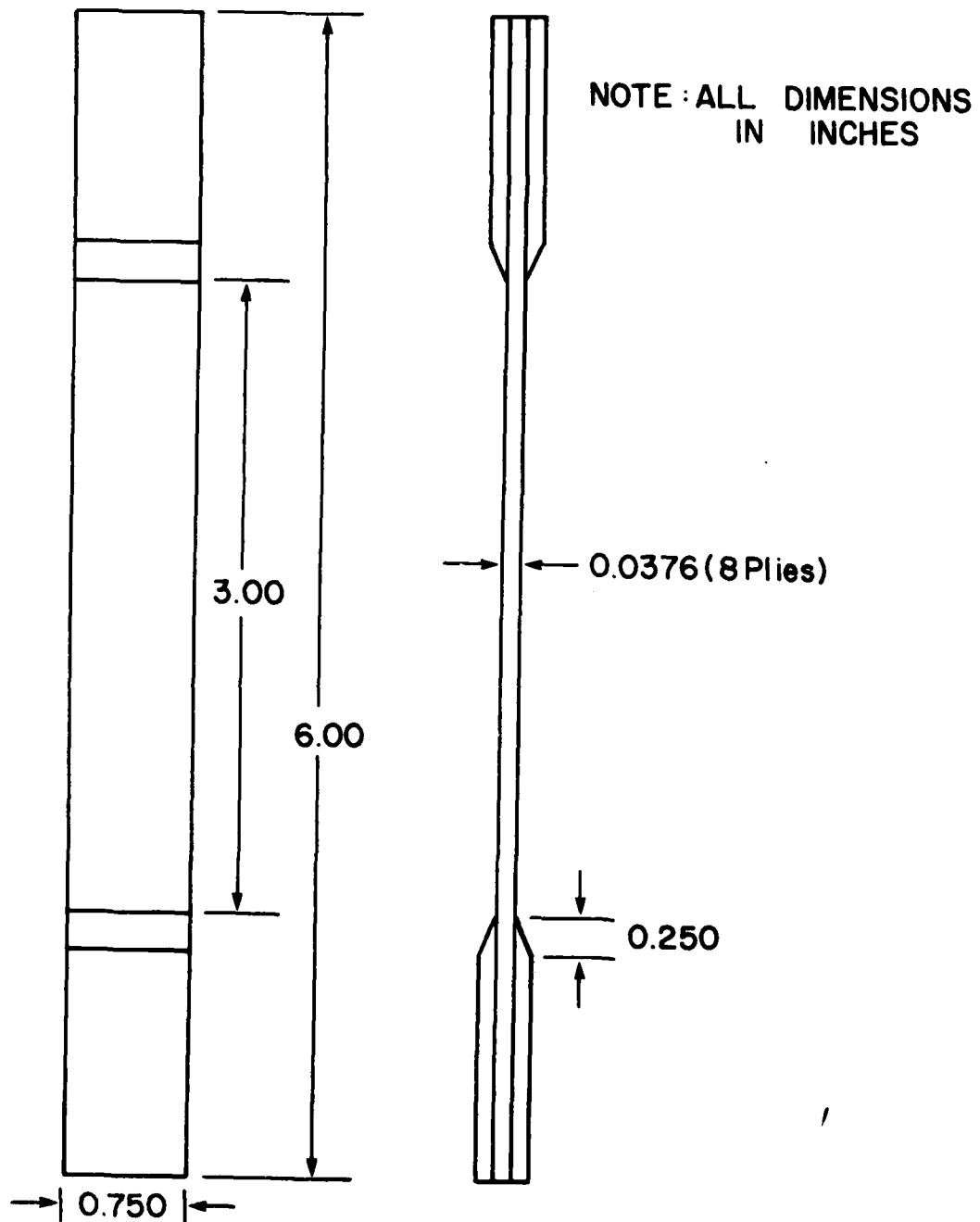
organic): (1) the specimens were 6 inches long rather than the Design Guide recommended 9 inches long and (2) the specimens were a nominal 3/4 inch wide rather than the Guide recommended 1 inch. The specimens used appear in Figures 3, 4, and 5 with nominal dimensions specified. These specimens were all instrumented on both sides with Micro-Measurements two element high resistance foil gages EP-08-125VB-120. The 0°B/Al specimen provides  $E_1$  and  $\nu_{12}$  (where 1 and 2 refer to material-axes orthogonal coordinate system with 1 taken along the fiber direction), the 90°B/Al provides  $E_2 (=E_3)$ , and the 0/90° SSWM provides  $E_1 (=E_2)$  and  $\nu_{12}$ .

### 2.3.2 Modified 10° Off-Axis Specimen

The 10° off-axis specimen<sup>(5)</sup> was selected to obtain the intralaminar shear modulus stress for boron/aluminum material. The recently developed specimen had several advantages over previously used specimens for intralaminar shear characterization. The discussion that follows includes (1) an indication of the origin of the specimen and the quality of results obtained from it, (2) a listing of some of the advantages and the disadvantages to using the specimen, and (3) the reasons the University selected the specimen for the test program described in this report.

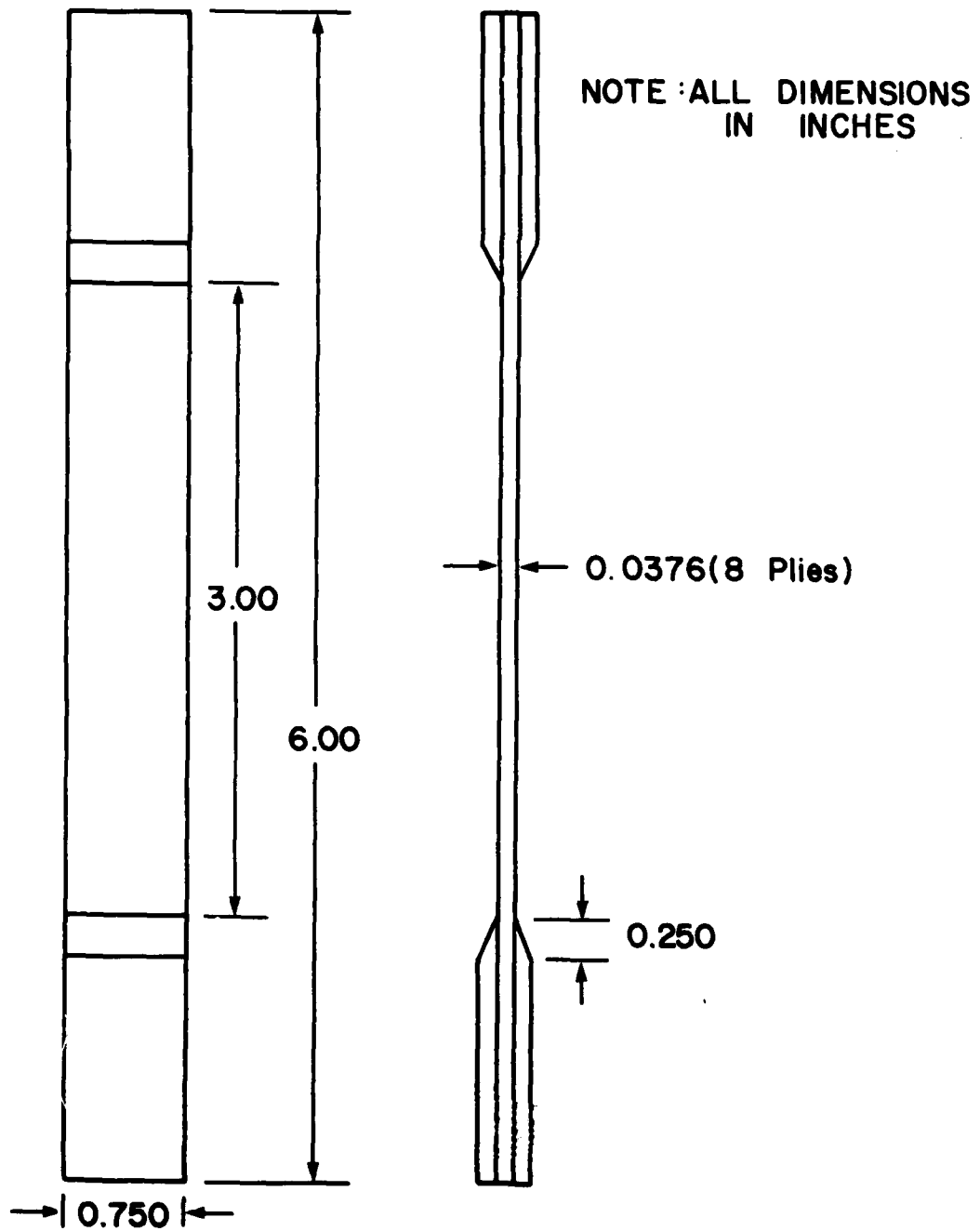
The specimen was developed and proposed by IITRI during a contractual study with NASA Lewis Research Center. A subsequent in depth theoretical and experimental investigation<sup>(5)</sup> yielded a satisfactory comparison of experimental and predicted curves. The results of that study prompted a recommendation that the specimen be considered as a standard test for intralaminar shear. The advantages of this specimen that were relevant to the current test program follow:

1. The specimens have uniform shear stress through the thickness.
2. The specimens are free of lamination residual stresses in contrast to the  $\pm 45^\circ$  specimen.
3. The use of the thin laminate narrow specimens saves considerable material (compared to thin tubes).



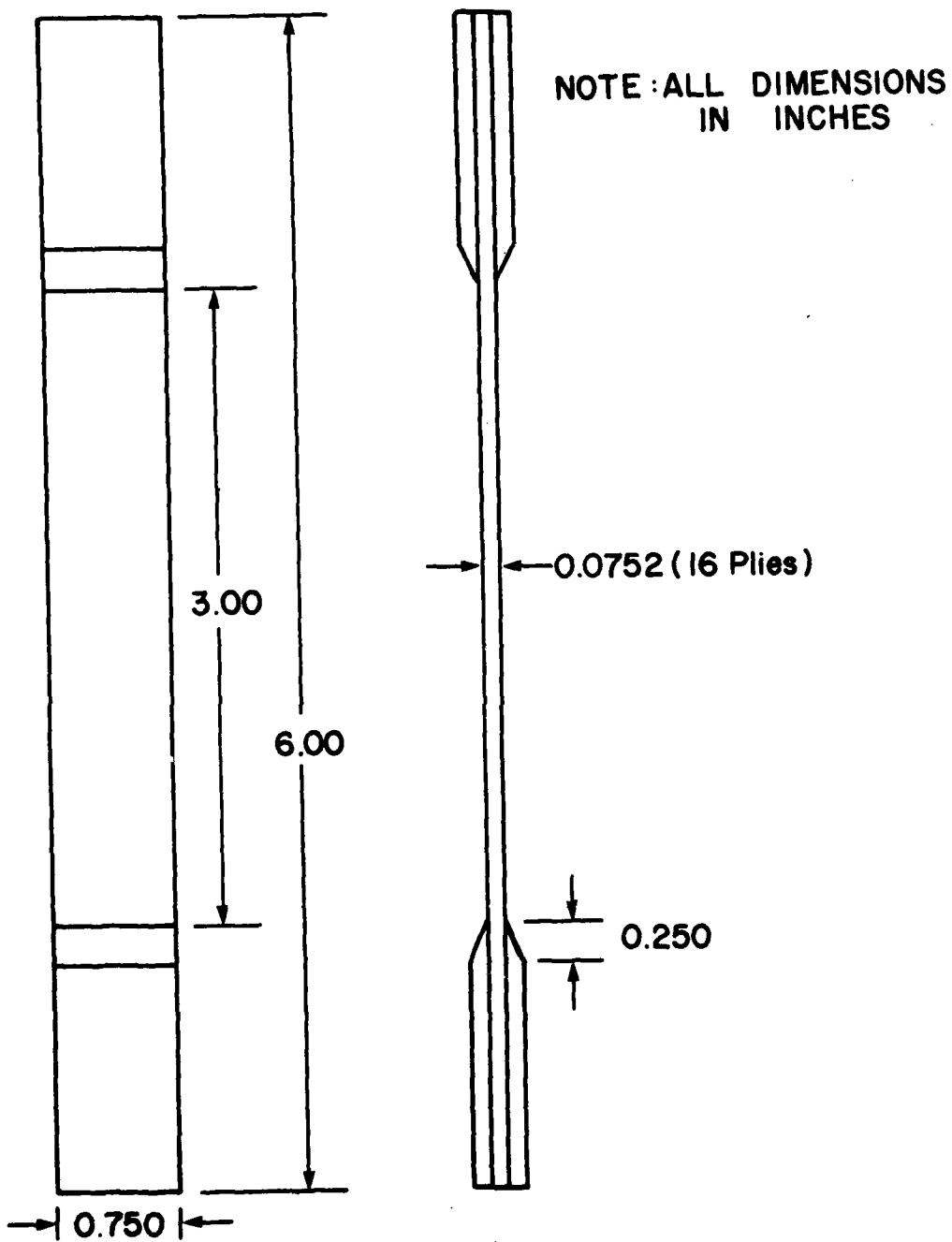
**0° BORON/2024 ALUMINUM SPECIMEN**

Figure 3. Specimen Configuration for 0° Boron/2024 Aluminum.



**90° BORON/2024 ALUMINUM SPECIMEN**

Figure 4. Specimen Configuration for 90° Boron/2024 Aluminum.



**0/90° STAINLESS STEEL  
WIRE MESH SPECIMEN**

Figure 5. Specimen Configuration for 0/90° Stainless Steel Wire Mesh/2024 Aluminum.

4. The specimens can be cut from the same laminate used to obtain specimens for longitudinal and transverse property characterization.
5. The use of a familiar tensile test procedure.

The disadvantages to using the specimen include:

1. An increase amount of data reduction calculations.
2. Increased care in aligning the specimen in the fixture and aligning the strain gages on the specimen.

The results of another study<sup>(6)</sup> which compared mechanical properties obtained from six different intralaminar shear specimen configurations were not as promising. However, the University of Dayton gave more weight to the study in Reference 5 because it was much more extensive experimentally and analytically than the Reference 6 study. The experiments for Reference 5 were conducted on three different materials whereas those for Reference 6 were conducted on one. Reference 6 contained no analysis of the specimen configuration. It contained only the results of data reduction.

Several factors strongly influenced the University's decision to use the specimen configuration. First, the advantages listed above made the specimen quite attractive. Second, predictable results had been obtained for the majority of tests conducted using the specimen. Third, the disadvantages to using the specimen were merely inconveniences. They were not problems associated with the fundamental design of the specimen which would produce erroneous results. Fourth, the program described in this report was to test metal matrix composite materials. Since all of the test cited above were conducted on epoxy based composites and most of them yielded acceptable and predictable results, the University anticipated that the specimen might be even more acceptable for testing metal matrix composites. Discussions of this latter point with T. Hahn and J. Whitney<sup>(7)</sup> (both of whom were at the Air Force Materials Laboratory at that time) reinforced the opinion that the specimen should work well with metal matrix composite materials.

The modified  $10^\circ$  off-axis specimen appears in Figure 6. The modifications, a 4 inch reduction in length and a  $3/8$  inch reduction in width, were justified by the fact that the matrix material was metallic rather than organic. B/Al specimens of the reduced size had been tested and predictable results obtained<sup>(8)</sup>. The specimens were instrumented with two Micro-Measurements, three element rosette strain gages, EA-08-125VB-120, placed back to back to cancel bending. The specimen provides  $G_{12}$  for the B/Al.

### 2.3.3 Through-the-Thickness Specimen

A through-the-thickness specimen was designed to obtain the elastic modulus in the interlaminar ( $E_3$ ) direction for the SSWM. The specimen appears in Figure 7. It was made by removing coins, a nominal 0.750 inches in diameter from a 136 ply thick layup of SSWM. (The fibers were perpendicular to the load axis.) Two inch long aluminum rods were attached to each end of the coin with a resin bond adhesive to provide an area to grip the specimen. Dowel pins through the holes in the grip section fasten the specimen in the test fixture. A reduced section was cut on the SSWM portion of the specimen. The specimen was instrumented with two Micro-Measurements EA-08-125AD-120 (single element) gages placed diametrically opposite each other and aligned with the direction of the applied load.

### 2.3.4 Torsion Rod Specimen

A torsion rod specimen was used to obtain the interlaminar shears  $G_{23}$  for the B/Al and  $G_{31}$  ( $=G_{23}$ ) for the SSWM. The specimens appear in Figures 8 and 9, respectively. They were made by removing coins, a nominal 0.700 inch in diameter, from a 135 ply thick layup of each material. Three of the coins (of one material) were diffusion bonded together to form a specimen having the fibers perpendicular to the long axis of the specimen. Four inch long aluminum bars were attached (resin bonded) to the fused specimens for use as grips.

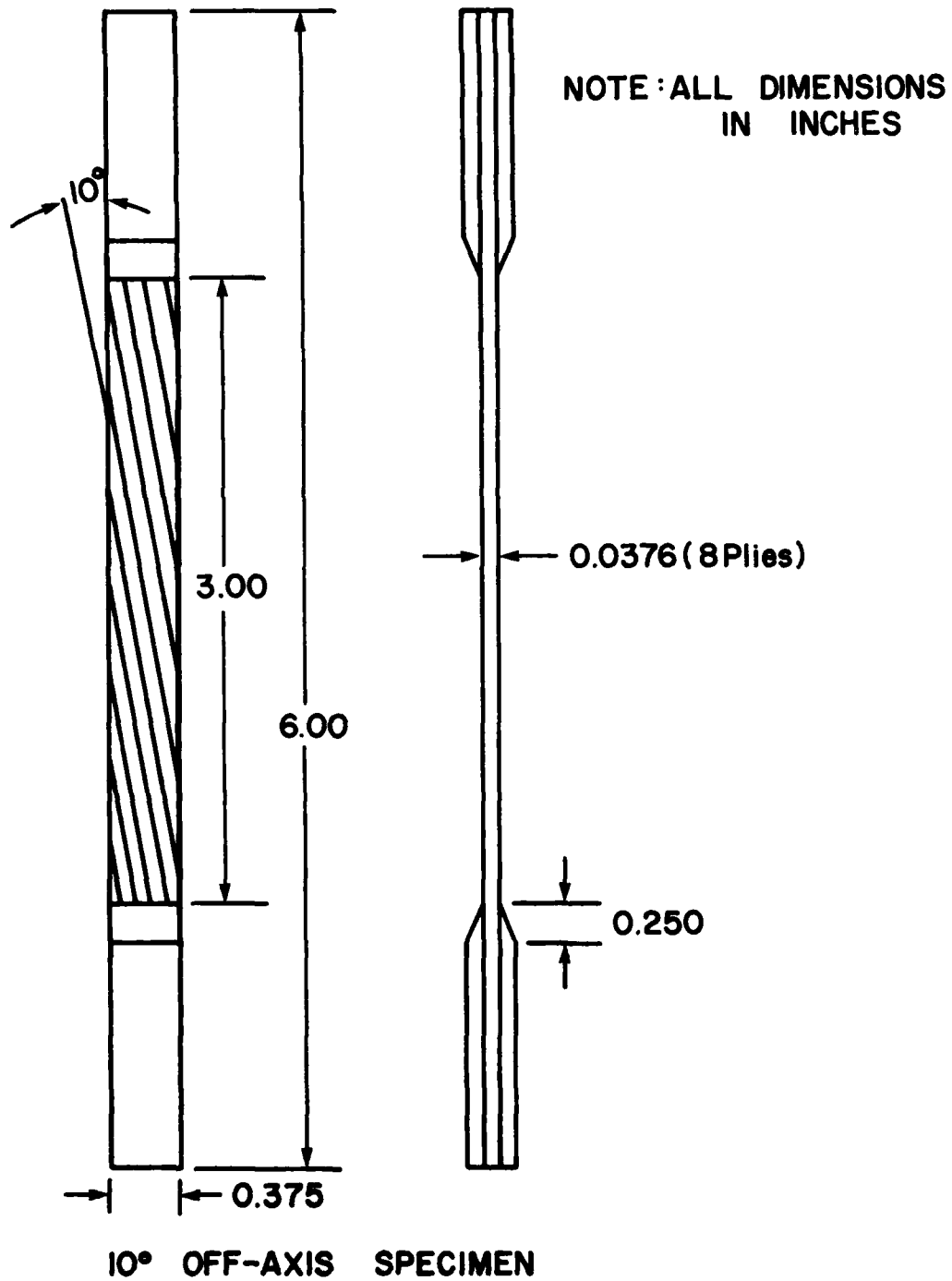
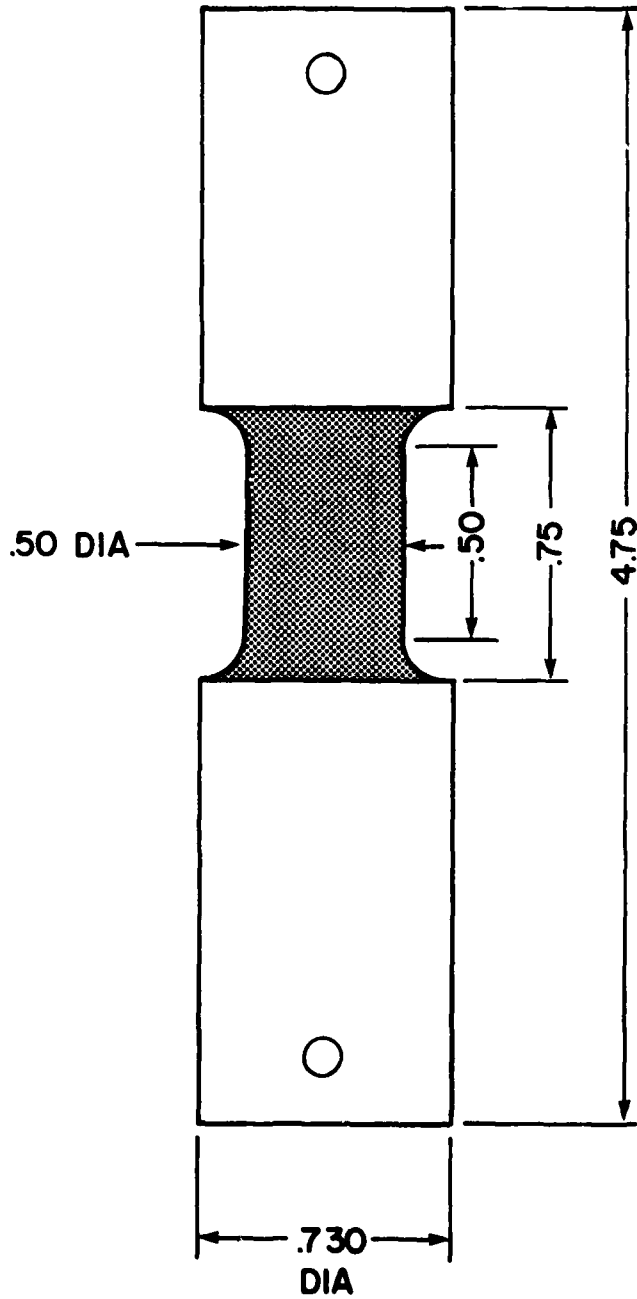


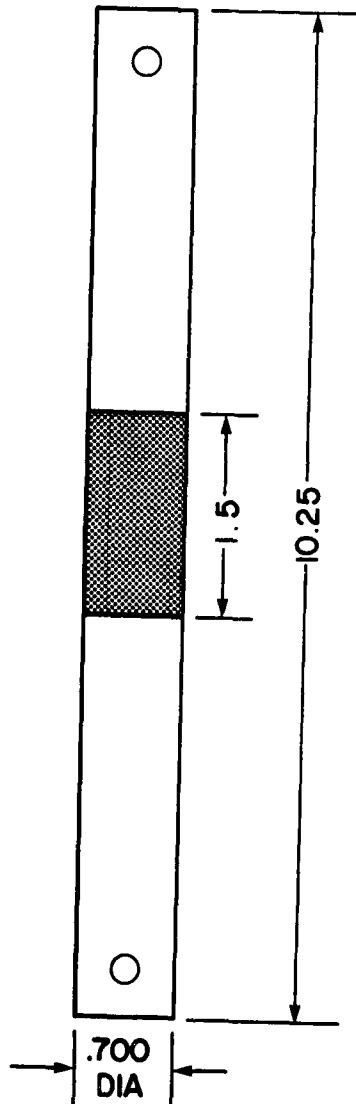
Figure 6. Specimen Configuration for 10° Off-Axis Boron/2024 Aluminum.



NOTE: ALL  
DIMENSIONS  
ARE IN INCHES

### THROUGH-THE-THICKNESS

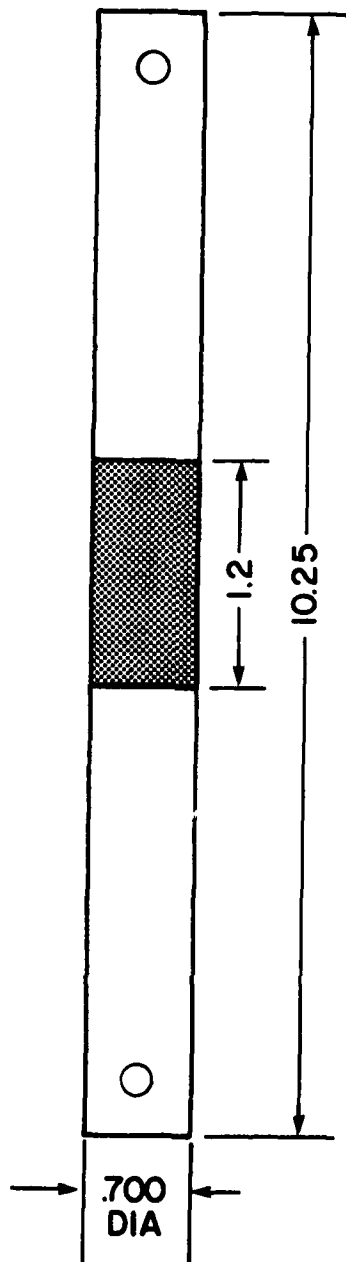
Figure 7. Specimen Configuration for Through-The-Thickness  
Stainless Steel Wire Mesh/2024 Aluminum.



NOTE: ALL  
DIMENSIONS  
ARE IN INCHES

**STAINLESS STEEL WIRE MESH  
TORSION ROD**

Figure 8. Specimen Configuration for Rod Torsion Stainless Steel Wire Mesh/2024 Aluminum.



NOTE: ALL  
DIMENSIONS  
ARE IN INCHES

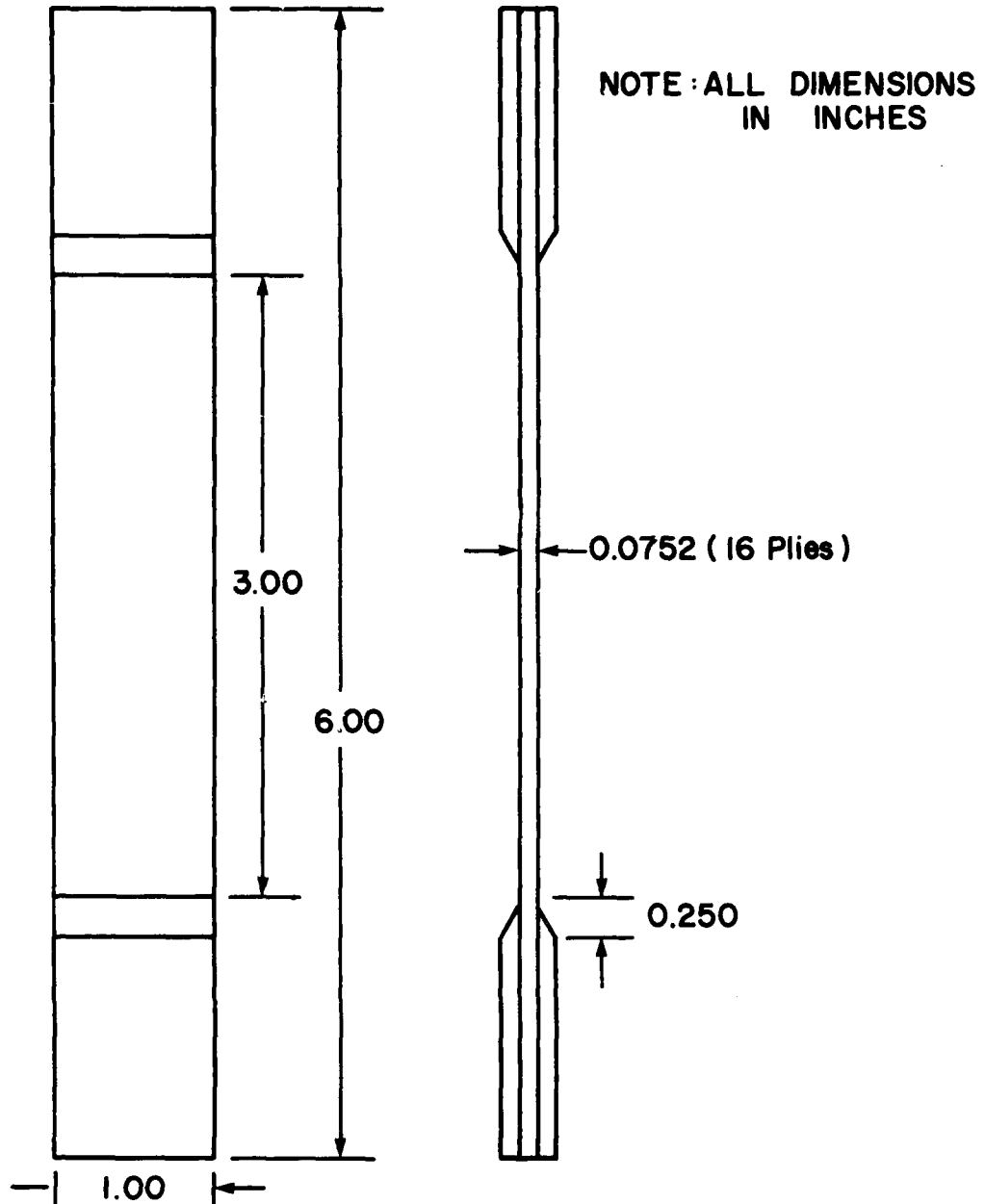
**BORON/ALUMINUM  
TORSION ROD**

Figure 9. Specimen Configuration for Rod Torsion Boron/2024 Aluminum.

The ASTM standard for torsion tests (E143) was consulted to determine the required length of the rods (so that one can assume that a uniform stress field exists in the test section). A dowel pin through the hole in each grip section fastens the specimen in the test fixture. A Micro-Measurements torsion gage, EP-08-125TD-120, was used on the specimen to obtain the strain data.

#### 2.3.5 $\pm 45^\circ$ Specimen

The standard  $\pm 45^\circ$  specimen was an obvious choice to obtain the intralaminar shear stress of the SSWM material because of the nature of the mesh. The specimen, shown in Figure 10, varies from the IITRI configuration (described above) only by the fiber direction. The nominal dimensions appear in the figure. The specimens were instrumented on both sides with Micro-Measurements two element foil gages, EP-08-125VB-120. The specimen provides  $G_{12}$  for the SSWM.



**±45° STAINLESS STEEL  
WIRE MESH SPECIMEN**

Figure 10. Specimen Configuration for ± 45° Stainless Steel Wire Mesh/2024 Aluminum.

SECTION III  
TEST FIXTURES AND EXPERIMENTAL PROCEDURES

This section contains photos of the test fixtures and system and discusses the experimental procedures for each test type. The test fixture and procedure descriptions are grouped under three headings. Each group comprises the test types conducted with one of three different test fixtures.

Each of the specimens, except for the torsion rod specimens, had two high resistance foil strain gages applied directly opposite each other to cancel any bending that might be present. The torsion rods had only one torsion gage applied. Each set of two individual gages (i.e., two Poisson, or two longitudinal, or two diametrically opposed elements of the three element rosette) was wired into two opposite legs of a Wheatstone Bridge circuit. The signal conditioner for the bridge output was a 218 Honeywell Bridge Amplifier. The medium rate load and strain data was recorded on the four channel transient Zonic recorder and played back onto the X-Y recorder. The quasi-static tests data was recorded directly on the X-Y recorder.

General Electric Company supplied the composite material specimens. The University measured the widths and thicknesses or the diameters of all specimens. These values were used in stress calculations and to document the uniformity of the specimens.

3.1 TEST FIXTURE AND PROCEDURES FOR THE 0° B/Al, 90° B/Al  
0-90° SSWM, 10° Off-Axis B/Al, ± 45° SSWM SPECIMEN

The 0° B/Al, 90° B/Al, 0-90° SSWM, 10° off-axis B/Al, and ± 45° SSWM specimens, all flat ones having aluminum tabs, were tested in the fixture shown in Figure 11. The test system consists of a set of Instron grips mounted in an electrohydraulic closed-loop test machine. The complete test system including the MTS control console appears in Figure 12. This test system



Figure 11. Test Fixture Used to Test All Flat Specimens With Specimen Installed.

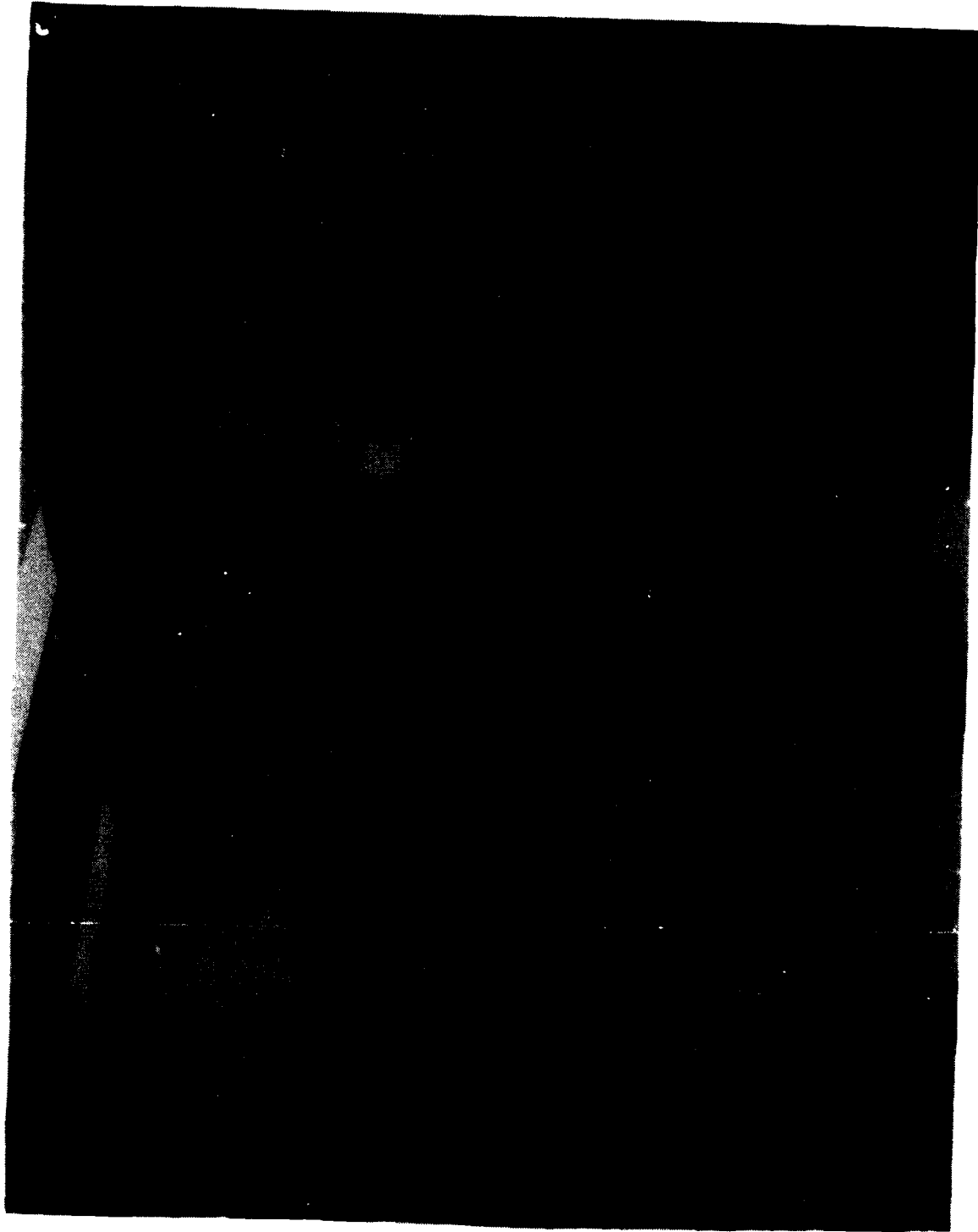


Figure 12. Entire Test System Used to Conduct All Tests for This Report Except the Rod Torsion Tests.

has the capability of being operated in load, strain, or displacement control. The tests described here were run in displacement control. Two of the 0° B/A1 tests were conducted at a displacement rate of 1 in/sec. The loads obtained were considerably smaller than had been expected. In resolving the problem a couple of tests were conducted at 0.001 in/sec. Values similar to those for the faster rate were obtained, consequently the remainder of the tests were conducted at the slower rate.

### 3.2 TEST FIXTURE AND PROCEDURES FOR THE THROUGH-THE-THICKNESS SPECIMENS

The fixture to test the through-the-thickness specimens appears in Figure 13 with a specimen installed. Dowel pins provide the mechanism for load application. All of these tests were run at a displacement rate of 0.001 in/sec. The control console and recording apparatus shown in Figure 12 completed this test system.

### 3.3 TEST FIXTURE AND PROCEDURES FOR THE SSWM AND B/A1 TORSION ROD SPECIMENS

The fixture used to test both the B/A1 and SSWM torsion rod specimens appears in Figure 14. The end plate (to the right in the photo) bolts to the base plate with spacers to form a rigid structure to hold the specimen. Dowel pins anchor the specimen in the fixture and provide the load path to apply the torque. The "end plate" end of the specimen remains fixed. The other end attaches to a spline in the base plate end of the fixture. A short arm attaches the rod which houses the spline to a hydraulic actuator. A strain gage bridge configured to measure the torque of the rod provides the control signal to the MTS control console. The torque, rotation and strain were each recorded directly on an X-Y recorder.

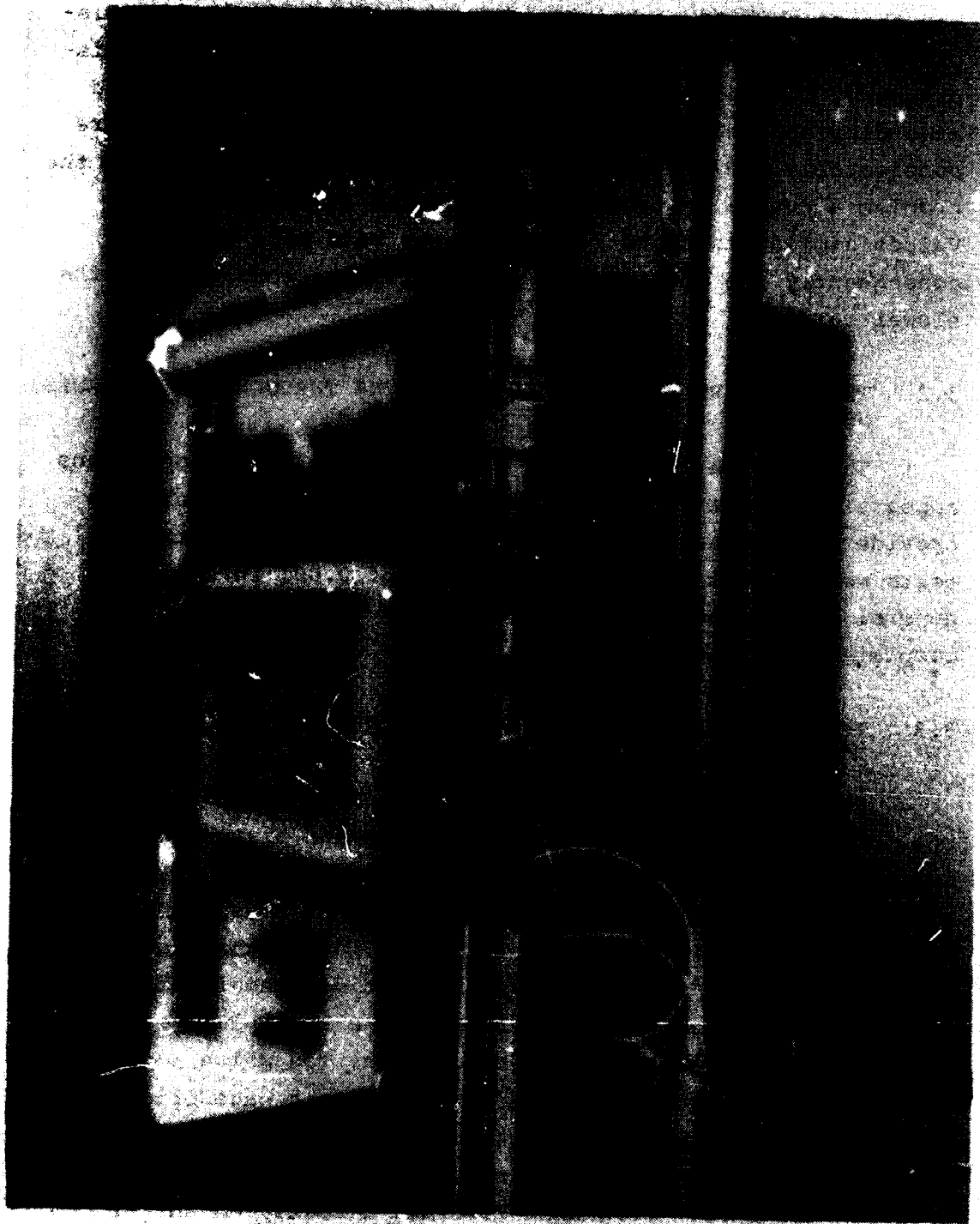


Figure 13. Test Fixture for Through-The-Thickness Specimen  
With Specimen Installed.



Figure 14. Test Fixture for Rod Torsion Tests Shown with Specimen Installed.

SECTION IV  
DATA REDUCTION

This section contains the data reduction relationships for the various test types. The parameters calculated using data from the appropriate test include the elastic modulus, the ultimate strength, the ultimate (percent) strain, the shear modulus and Poisson's ratio. In all cases engineering parameters were calculated (rather than true stress and strain). The reduced data appears in Section V.

4.1 MODIFIED IITRI SPECIMEN (0° B/A1, 90° B/A1, and 0/90° SSWM)

The data reduction for the 0° and 90° B/A1 and the 0/90° SSWM was straightforward. The elastic modulus, the ultimate strength, the ultimate strain (percent), and Poisson's ratio for the 1 and 2 material directions were calculated using the following relationships:

$$E_{1(\text{and } 2)} = \frac{\sigma_e}{\epsilon_e} = \frac{P/A}{\epsilon_e}$$

$$\sigma_{\text{ult}} = \frac{P_{\text{max}}}{A}$$

$$\epsilon_{\text{ult}} (\%) = \epsilon_{e(\text{max})} \times 100$$

$$\nu_{12} = -\frac{\epsilon_t}{\epsilon_l}$$

where: E = elastic moduli in the 1 and 2 material direction  
 $\sigma_e$  = engineering stress  
 $\epsilon_e$  = engineering strain in the longitudinal direction  
P = load  
 $P_{\text{max}}$  = maximum load

$A$  = crosssectional area of the specimen  
 $\epsilon_{ult}$  = ultimate strain in percent  
 $\nu$  = Poisson's ratio  
 $\epsilon_t$  = transverse strain  
 $\epsilon_l$  = longitudinal strain

$E_1$ ,  $E_2$ ,  $\sigma_{ult1}$ ,  $\epsilon(\%)_{ult1}$ ,  $\sigma_{ult2}$ ,  $\epsilon(\%)_{ult2}$ ,  $\nu_{12}$ , and  $\nu_{21}$  were calculated for the B/A1 from these tests.  $E_1 (=E_2)$ ,  $\sigma_{ult1} (= \sigma_{ult2})$ ,  $\epsilon(\%)_{ult1} (= \epsilon(\%)_{ult2})$ , and  $\nu_{12} (= \nu_{21})$  were calculated for the SSWM.

#### 4.2 $\pm 45^\circ$ SSWM SPECIMEN

Data reduction for the  $\pm 45^\circ$  SSWM specimen yields the intralaminar shear modulus,  $G_{12}$ . P.H. Petit<sup>(9)</sup> presents relationships that utilize elastic constants from uniaxial tests in the transverse and longitudinal directions in addition to the tangent modulus, and the longitudinal and transverse strains of the  $\pm 45^\circ$  stress-strain curves. An incremental shear stress-strain curve for the constituent laminae results from the calculations. The equations follow:

$$G_{12} = \frac{2U_1 E_{xx}^{+45}}{8U_1 - E_{xx}^{+45}}$$

$$\gamma_{12} = (1 + \nu_{xy}) \epsilon_x$$

and

$$\Delta\tau_{12} = G_{12} \gamma_{12}$$

where

$$U_1 = \frac{1}{8(1 - \nu_{12} \nu_{21})} [E_1 + E_2 + 2\nu_{21} E_1]$$

and

$$\nu_{21} = \nu_{12} \frac{E_2}{E_1}$$

However,  $E_1$  and  $E_2$  were assumed to be equal for these experiments so  $\nu_{21} = \nu_{12}$  and  $U_1 = E_1/4(1 - \nu_{12})$ . (All of the data was obtained from laminates of the same thickness consequently the fiber volume was the same for the unidirectional and  $\pm 45^\circ$  data, an important factor in the use of these equations.) The shear modulus was the initial tangent of the incremental shear stress-strain curve.

#### 4.3 THROUGH-THE-THICKNESS SPECIMEN

The data reduction for the through-the-thickness specimen was straightforward. The parameter of interest was  $E_3$  for the SSWM. The equations follow:

$$E_3 = \frac{\sigma_e}{\epsilon_e} = \frac{P/A}{\epsilon_e}$$

where:  $E_3$  = elastic modulus in the three material direction

$\sigma_e$  = engineering stress

$\epsilon_e$  = engineering strain

P = load

A = crosssectional area of the specimen

The ultimate stress and strain couldn't be calculated for these specimens because they failed at the bond between the tab end and the test specimen section. Poisson's ratio could not be calculated for this specimen because it was not possible to locate the exact orientation of the fibers in the specimen, i.e., one could not determine the location on the circumference to place the longitudinal and transverse strain gages.

#### 4.4 10° OFF-AXIS SPECIMEN

The 10° off-axis specimen provides data to calculate  $G_{12}$  for the boron aluminum material. The equation relating the strain gage strains to the structural axes (x and y of the specimen) strains follows:

$$\begin{Bmatrix} \epsilon_{g1} \\ \epsilon_{g2} \\ \epsilon_{g3} \end{Bmatrix} = \begin{Bmatrix} \cos^2 \theta_{g1} & \sin^2 \theta_{g1} & \frac{1}{2} \sin 2\theta_{g1} \\ \cos^2 \theta_{g2} & \sin^2 \theta_{g2} & \frac{1}{2} \sin 2\theta_{g2} \\ \cos^2 \theta_{g3} & \sin^2 \theta_{g3} & \frac{1}{2} \sin 2\theta_{g3} \end{Bmatrix} \begin{Bmatrix} \epsilon_{cxx} \\ \epsilon_{cyy} \\ \epsilon_{cxy} \end{Bmatrix}$$

where:  $\epsilon_{g1}$ ,  $\epsilon_{g2}$ ,  $\epsilon_{g3}$  denote the true (measured strains corrected for gage transverse sensitivity) strain from gages 1, 2, and 3 respectively.

$\theta_{g1}$ ,  $\theta_{g2}$ ,  $\theta_{g3}$  denote the corresponding orientation angles measured from the load directions

$\epsilon_{cxx}$ ,  $\epsilon_{cyy}$ ,  $\epsilon_{cxy}$  denote the structural axes strains

The equation

$$\epsilon_{\lambda 12} = (\epsilon_{cyy} - \epsilon_{cxx}) \sin 2\theta + \epsilon_{cxy} \cos 2\theta$$

relates the structural-axes strain to ply intralaminar shear strain for any orientation  $\theta$ . The equation relating the ply intralaminar shear stress to the structural-axes stress is:

$$\sigma_{\lambda 12} = 0.171 \sigma_{cxx}$$

These equations appear in Reference 5 with a more detailed description of their development.

The gage configuration for the tests conducted for this report was  $\theta_{g1} = 135^\circ$ ,  $\theta_{g2} = 90^\circ$ , and  $\theta_{g3} = 45^\circ$ . Inserting these values in the coefficient matrix above and reducing the equations results in the following equations for intralaminar shear strain:

$$\epsilon_{\lambda 12} = -1.282 \epsilon_{g1} + 0.684 \epsilon_{g2} + 0.591 \epsilon_{g3}$$

The intralaminar shear stress-strain curve was generated as follows: For each load increment,

- (1) Use the equation immediately above to calculate  $\epsilon_{\ell 12}$
- (2) Use the equation preceeding that to calculate  $\sigma_{\ell 12}$
- (3) Plot  $\sigma_{\ell 12}$  against  $\epsilon_{\ell 12}$  for each load increment

The initial ply shear modulus,  $G_{12}$ , was determined from the slope of the initial tangent to the curve generated in (3).

#### 4.5 TORSION ROD SPECIMENS

The relationship for reducing the data from the rod torsion tests was derived using Saint-Venant torsion theory. (The extension rods attached to the test section of the specimen were long enough that one could assume a uniform stress distribution in the test section.) The equation used was:

$$\frac{2\xi}{\xi + 1} = \frac{TL}{G_{12}J\theta}$$

- where:
- $\xi = G_{23}/G_{12}$
  - $T =$  applied torque
  - $L =$  length of rod section to which the torque was applied
  - $G_{12} =$  shear modulus on a plane
  - $J =$  polar moment of inertia of the specimen cross section
  - $\theta =$  angle of twist, in radians

$G_{12}$  was obtained for both the B/Al and SSWM from a separate test, consequently, the above equation yielded  $G_{23}$  for each of the materials.

SECTION V  
RESULTS AND CONCLUSIONS

This section presents and discusses the test results. The calculated mechanical properties obtained from the test data for the B/Al and SSWM appear in Tables 2 through 9. Tables 6 and 7 also contain recorded data points and the points of an incremental stress-strain curve generated from the recorded data. Table 2 summarizes the results by presenting the primary and shear moduli and Poisson's ratio for each of the materials. Most of the values in Table 2 represent the average of the results of three tests. The materials tested had a fiber volume content of approximately 40 percent.

TABLE 2. AVERAGE ELASTIC MECHANICAL PROPERTIES FOR B/2024 Al AND SSWM/2024 Al.

Mechanical Property	Material	
	B/Al	SSWM
$E_1$	$27.0 \times 10^6$ psi	$15.3 \times 10^6$ psi
$E_2$	$15.7 \times 10^6$ psi	$15.3 \times 10^6$ psi
$E_3$	$15.7 \times 10^6$ psi	$7.4 \times 10^6$ psi
$G_{12}$	$6.9 \times 10^6$ psi	$5.6 \times 10^6$ psi
$G_{23}$	$1.5 \times 10^6$ psi	$1.5 \times 10^6$ psi
$G_{31}$	$6.9 \times 10^6$ psi	$1.5 \times 10^6$ psi
$\nu_{12}$	.23	.31
$\nu_{21}$	.12	.31

Some of the mechanical properties for the B/Al did not compare well with values found in the literature. Some of the values obtained here were comparable to literature values. The elastic moduli in the one and two material directions were

TABLE 3. RESULTS FROM 0° B/Al MODIFIED IITRI SPECIMEN

Specimen	E <sub>1</sub> Modulus (psi x 10 <sup>6</sup> )	Ultimate Strength (psi x 10 <sup>3</sup> )	Ultimate Strain (percent ε)	ν <sub>12</sub> Poisson's Ratio
B4-1	27.7	56.4	0.26	*
B4-3	25.6	*	*	0.23
B4-2	28.2	47.0	0.18	0.23
B4-4	26.6	58.9	*	0.25

\* Not Available

NOTE: Ultimate strength and strain were calculated using the maximum load and strain at failure. Failure occurred near the tab, about one inch from the strain gage location so the actual fracture strain was larger.

TABLE 4. RESULTS FROM 90° B/Al MODIFIED IITRI SPECIMEN

Specimen	E <sub>2</sub> (=E <sub>3</sub> ) Modulus (psi x 10 <sup>6</sup> )	Ultimate Strength (psi x 10 <sup>3</sup> )	Ultimate Strain (percent ε)	Poisson's Ratio
B6-2	15.7	17.2	0.20	0.139
B6-3	16.0	18.6	0.27	0.148
B7-2	15.5	18.7	0.27	0.08

NOTE: Ultimate strength and strain were calculated using the maximum load and strain at failure. Failure occurred near the tab, about one inch from the strain gage location so the actual fracture strain was larger.

TABLE 5. RESULTS FROM 0/90° SSWM MODIFIED IITRI SPECIMEN

Specimen	E <sub>1</sub> (=E <sub>2</sub> ) Modulus (psi x 10 <sup>6</sup> )	Ultimate Strength (psi x 10 <sup>3</sup> )	Ultimate Strain (percent ε)	Poisson's Ratio
M3-2	15.0	44.9	2.9	0.33
M2-1	15.6	46.3	2.8	0.28
M3-3	15.3	42.9	2.0	0.35

NOTE: Ultimate strength and strain were calculated using the maximum load and strain at failure. Failure occurred near the tab, about one inch from the strain gage location so the actual fracture strain was larger.

TABLE 6. RESULTS FROM THE THROUGH-THE-THICKNESS SPECIMEN

Specimen	E <sub>3</sub> Modulus (psi x 10 <sup>6</sup> )
M7-1	6.2
M7-6	7.7
M7-8	7.5

NOTE: Ultimate strength and strain could not be obtained for these tests because failure occurred at the resin bond between the test section and the attached grip section.

TABLE 7. RAW AND REDUCED DATA FROM  $\pm 45^\circ$  SSMM SPECIMEN

Specimen	Increment	Raw Test Data						Calculated Incremental Shear Stress-Strain Curve Values		
		$\sigma_x$ psi	$\epsilon_x$ in/in	$\epsilon_y$ in/in	$E_{xx}$ $\times 10^6$ psi	$\nu_{xy}$	$G_{12}$ $\times 10^6$ psi	$\gamma_{12}$ in/in	$\tau_{12}$ $\times 10^3$ psi	
M5-1	1	11689	.0005	.0018	23.38	.350	12.30	.00068	8.36	
	2	15585	.0010	.0055	15.58	.550	5.99	.00160	9.58	
	3	17711	.0015	.0088	11.80	.583	4.01	.00238	9.55	
	4	19482	.0020	.0133	9.74	.662	3.12	.00333	10.40	
	5	21423	.0025	.0173	8.56	.690	2.65	.00423	11.20	
	6	24086	.0035	.0244	6.88	.697	2.03	.00600	12.20	
	7	26212	.0045	.0313	5.82	.694	1.67	.00760	12.70	
	8	28691	.0055	.0388	5.22	.705	1.48	.00940	13.90	
	9	31879	.0080	.0573	3.98	.716	1.09	.01389	15.10	
	10	33296	.0100	.0690	3.50	.721	0.95	.01640	15.60	
	11	35067	.0120	.0870	2.92	.721	0.78	.02070	16.20	
M4-2	1	8954	.0005	.0015	17.91	.300	7.49	.00065	4.87	
	2	13969	.0010	.0040	13.97	.400	5.09	.00140	7.12	
	3	16476	.0015	.0075	10.98	.500	3.64	.00225	8.20	
	4	18267	.0020	.0113	9.13	.565	2.87	.00313	9.00	
	5	19699	.0025	.0138	7.88	.552	2.39	.00388	9.29	
	6	21490	.0030	.0183	7.16	.610	2.13	.00483	10.30	
	7	25072	.0043	.0263	5.83	.612	1.68	.00693	11.60	
	8	27579	.0055	.0350	5.01	.636	1.41	.00900	12.70	
	9	30086	.0073	.0465	4.12	.637	1.14	.01195	13.60	
	10	34026	.0120	.0738	2.84	.615	0.76	.01938	14.70	
	11	36891	.0183	.1088	2.02	.595	0.53	.02919	15.40	
M5-2	1	7489	.0005	.0030	14.98	.600	5.64	.00080	4.51	
	2	13909	.0010	.0050	13.91	.500	5.06	.00150	7.58	
	3	16762	.0015	.0085	11.18	.567	3.73	.00235	8.77	
	4	18716	.0020	.0120	9.36	.600	2.96	.00320	9.48	
	5	20337	.0025	.0150	8.13	.600	2.49	.00400	9.94	
	6	23191	.0035	.0205	6.63	.586	1.95	.00555	10.81	
	7	25849	.0045	.0285	5.75	.633	1.65	.00735	12.10	
	8	28531	.0064	.0375	4.46	.586	1.24	.01015	12.60	
	9	31384	.0083	.0510	3.78	.615	1.03	.01340	13.80	
	10	34237	.0010	.0710	3.11	.646	0.84	.01811	15.10	
	11	36733	.0168	.1090	2.19	.589	0.58	.02669	15.40	

SPECIMEN SHEAR MODULUS  
M4-2 4.85 x 10<sup>6</sup> psi  
M5-1 7.50 x 10<sup>6</sup> psi  
M5-2 4.30 x 10<sup>6</sup> psi

TABLE 8. RECORDED AND REDUCED DATA FROM 10° OFF-AXIS B/A1 SPECIMENS.

SPECIMEN	RECORDED DATA				REDUCED DATA	
	P	2 $\epsilon_{q1}$	2 $\epsilon_{q2}$	2 $\epsilon_{q3}$	$\sigma_{\ell 12}$	$\epsilon_{\ell 12}$
	lbs	$\mu\epsilon$	$\mu\epsilon$	$\mu\epsilon$	psi	$\mu\epsilon$
B2-1	100	212.5	- 100	+125	948	- 133
	200	412.5	- 225	+250	1895	- 267
	300	625	- 344	+350	2843	- 414
	400	850	- 469	+465	3791	- 566
	500	1137	- 625	+575	4738	- 771
	600	1500	- 825	+675	5686	-1042
	700	1962	-1112	+695	6634	-1430
	800	2550	-1500	+600	7581	-1968
B2-2	100	188	- 53	119	950	- 105
	200	388	- 200	225	1900	- 249
	300	612	- 338	312	2851	- 415
	400	838	- 488	388	3801	- 588
	500	1125	- 688	425	4751	- 829
	600	1450	- 912	412	5702	-1118
	700	1875	-1200	325	6652	-1515
B2-3	100	238	- 125	112	941	- 144
	200	438	- 238	225	1881	- 388
	300	650	- 350	325	2822	- 417
	400	888	- 475	478	3763	- 613
	500	1188	- 612	531	4703	- 812
	600	1625	- 800	562	5644	-1147
	700	2112	-1088	500	6585	-1576
B2-4	125	200	- 175	+87.5	1201	- 162
	250	450	- 375	187.5	2402	- 361
	375	750	- 950	225	4804	- 963
	625	1600	-1325	100	6005	-1449
	750	2325	-1825	100	7206	-2085

SPECIMEN

SHEAR MODULUS

B2-1	$G_{12} = 6.9 \times 10^6$ psi
B2-2	$G_{12} = 8.2 \times 10^6$ psi
B2-3	$G_{12} = 5.9 \times 10^6$ psi
B2-4	$G_{12} = 6.7 \times 10^6$ psi

TABLE 9. RECORDED DATA AND CALCULATED RESULTS FROM TORSION ROD SPECIMEN

Specimen	Torque (in-lb)	Rotation Radians	$G_{23}$ Shear Modulus $\times 10^6$ psi
SSWM M8-1	150	0.02247	1.46
SSWM M8-2	150	0.02247	1.46
SSWM M8-3	150	0.02138	1.55
SSWM M8-4	150	0.02138	1.55
B/A1-1	150	0.02217	1.41
B/A1-2	150	0.02147	1.47
B/A1-3	150	0.01937	1.67

slightly below the literature values. No values for  $E_3$  were found for comparison to the values here. The Poisson's ratios compare well with literature values. In addition,  $\nu_{21}$  calculated from the average values of  $\nu_{12}$ ,  $E_1$  and  $E_2$  was nearly the same as the average of the  $\nu_{21}$  values obtained experimentally. The shear modulus  $G_{12}$  ( $=G_{31}$ ) compares well with Reference 8. No values were found for comparison to  $G_{23}$ . The ultimate strength obtained here was about one third as large as had been found in the literature. The ultimate strain was smaller than literature values; however, one would expect that because the specimens failed near the tab, almost an inch away from the strain gage. No ultimate shear strengths could be obtained because (1) the intralaminar shear test specimens had premature tensile failures and (2) the intralaminar shear tests were limited by the resin bond.

It was not possible to compare the mechanical properties obtained here for SSWM because no data for the material was found in the literature. It should be noted that the ultimate strain shown here was measured nearly an inch away from the failure location (because the specimen failed near the tab). The ultimate strength and strain could not be obtained from the through-the-thickness tests because the specimen failed at the resin bond. The intralaminar shear specimens did not fail so no ultimate shear strength could be calculated. For this material, as for the B/Al, the intralaminar shear tests was limited by the resin bond.

In conclusion, the mechanical properties obtained for the B/Al indicate that the material tested for this study was different than had been tested in previous studies. No comparable statement can be made about the SSWM because no data was found in the literature.

SECTION IV  
REFERENCES

1. NASA CR-135086.
2. Meyn, D.A., "Effect of Temperature and Strain Rate on the Tensile Properties of Boron-Aluminum and Boron-Epoxy Composites," Composite Materials Testing and Design (Third Conference), ASTM STP 546, 1974, pp. 225-236.
3. Green, S.J. and S.G. Babcock, "Response of Materials to Suddenly Applied Stress Loads: Part I: High Strain-rate Properties of Eleven Reentry-vehicle Materials at Elevated Temperatures," TR 66-83, Part I, November 1966.
4. Krinke, D.C., J.P. Barber, and T. Nicholas, "The Charpy Impact Tests as a Method for Evaluating Impact Resistance of Composite Materials," UDRI-TR-77-54.
5. Chamis, C.C. and J.H. Sinclair, "Ten-Degree Off-Axis Test for Shear Properties in Fiber Composites," Experimental Mechanical, September 1977, pp. 339-346.
6. Chiao, C.C., R.L. Moore, and T.T. Chiao, "Measurements of Shear Properties of Fiber Composites Part I, Evaluation of Test Methods," Composites, July 1977, pp. 161-174.
7. Private Communication with T. Hahn and J. Whitney.
8. Private Communication with C.C. Chamis.
9. Petit, P.H., "A Simplified Method of Determining In-Plane Shear Stress-Strain Response of Unidirectional Composites," Composite Materials Testing and Design, ASTM STP 460, pp. 83-93.

TABLE 7. RAW AND REDUCED DATA FROM  $\pm 45^\circ$  SSWM SPECIMEN

Specimen	Increment	Raw Test Data					Calculated Incremental Shear Stress-Strain Curve Values				
		$\sigma_x$ psi	$\epsilon_x$ in/in	$\epsilon_y$ in/in	$E_{xx}^{+45}$ psi	$\nu_{xy}$	$G_{12} \times 10^6$ psi	$\gamma_{12}$ in/in	$\tau_{12} \times 10^3$ psi		
M5-1	1	11689	.0035	.00018	23.38	.350	12.30	.00068	8.36		
	2	15585	.0010	.00055	15.58	.550	5.99	.00160	9.58		
	3	17711	.0015	.00088	11.80	.583	4.01	.00238	9.55		
	4	19482	.0020	.00133	9.74	.662	3.12	.00333	10.40		
	5	21423	.0025	.00173	8.56	.690	2.65	.00423	11.20		
	6	24086	.0035	.00244	6.88	.697	2.03	.00600	12.20		
	7	26212	.0045	.00313	5.82	.694	1.67	.00760	12.70		
	8	28691	.0055	.00388	5.22	.705	1.48	.00940	13.90		
	9	31879	.0080	.00573	3.98	.716	1.09	.01389	15.10		
	10	33296	.0100	.00690	3.50	.721	0.95	.01640	15.60		
	11	35067	.0120	.00870	2.92	.721	0.78	.02070	16.20		
M4-2	1	8954	.0005	.00015	17.91	.300	7.49	.00065	4.87		
	2	13969	.0010	.00040	13.97	.400	5.09	.00140	7.12		
	3	16476	.0015	.00075	10.98	.500	3.64	.00225	8.20		
	4	18267	.0020	.00113	9.13	.565	2.87	.00313	9.00		
	5	19699	.0025	.00138	7.88	.552	2.39	.00388	9.29		
	6	21490	.0030	.00183	7.16	.610	2.13	.00483	10.30		
	7	25072	.0043	.00263	5.83	.612	1.68	.00693	11.60		
	8	27579	.0055	.00350	5.01	.636	1.41	.00900	12.70		
	9	30086	.0073	.00465	4.12	.637	1.14	.01195	13.60		
	10	34026	.0120	.00738	2.84	.615	0.76	.01938	14.70		
	11	36891	.0183	.01088	2.02	.595	0.53	.02919	15.40		
M5-2	1	7489	.0005	.00030	14.98	.600	5.64	.00080	4.51		
	2	13909	.0010	.00050	13.91	.500	5.06	.00150	7.58		
	3	16762	.0015	.00085	11.18	.567	3.73	.00235	8.77		
	4	18716	.0020	.00120	9.36	.600	2.96	.00320	9.48		
	5	20337	.0025	.00150	8.13	.600	2.49	.00400	9.94		
	6	23191	.0035	.00205	6.63	.586	1.95	.00555	10.81		
	7	25849	.0045	.00285	5.75	.633	1.65	.00735	12.10		
	8	28531	.0064	.00375	4.46	.586	1.24	.01015	12.60		
	9	31384	.0083	.00510	3.78	.615	1.03	.01340	13.80		
	10	34237	.0010	.00710	3.11	.646	0.84	.01811	15.10		
	11	36733	.0168	.00990	2.19	.589	0.58	.02669	15.40		

SPECIMEN SHEAR MODULUS  
M4-2 4.85 x 10<sup>6</sup> psi  
M5-1 7.50 x 10<sup>6</sup> psi  
M5-2 4.30 x 10<sup>6</sup> psi

LATE  
LME